

## Heat Transport Processes at the KTB<sup>1</sup>

Christoph Clauser\*, Ulrich Harms<sup>§</sup>, Ernst Huenges<sup>§</sup>, Thomas Kohl<sup>#</sup>, Holger Lehmann\*, and  
Ladislaus Rybach<sup>#</sup>

<sup>#</sup>ETH (Zürich), <sup>§</sup>GFZ (Potsdam), <sup>\*</sup>NLFB-GGA (Hannover), <sup>§</sup>NLFB-KTB (Hannover)

### Introduction

Gaining a better insight into crustal heat transport processes was one of the main targets of the KTB-project. However, in the course of the project specific answers to very practical questions were expected from the heat flow community as well, such as predictions of the expected temperature in the next drilled section of the borehole. Thus geothermics was expected to "look ahead of the bit", like maybe only reflection seismology, and predictions of technical and operational relevance were demanded on temperature, its gradient, and heat flow density. And these predictions were eventually going to be confirmed or falsified. Both this high claim, and the search for reasons for past mispredictions turned out extremely stimulating for geothermal research. However, one general problem is in the discrepancy between this ambitious task on the one hand, and the amount and quality of available temperature data on the other. In part this is inevitable: drilling disturbs the temperature field vigorously and, even more important, for a long time. Sufficient thermal recovery requires a multiple of the drilling (and circulation) time. Many years will therefore pass until the thermal disturbances in the KTB main hole (HB) will have sufficiently died out. Meanwhile, the only temperature data available from the HB are extrapolations to undisturbed conditions from repeat measurements during comparatively short drilling breaks: bottom-hole temperatures (BHT) on seven depth levels in total and continuous temperature logs. Unfortunately, the KTB pilot hole (VB) has only been accessible to a depth of 2 km since December 1990 due to a stuck and abandoned hydraulic packer. This comparatively short interval is therefore to date the only source of temperature data of good quality for the KTB project. To illustrate this dilemma, maybe a comparison with reflection seismology is illuminating: what interpretations could be made if only one single and incomplete geophone trace and additionally some approximations of some other reflections were available instead of the complete wave-field of a reflection profile?

---

<sup>1</sup>written version of a plenary paper given on the occasion of the 7th. KTB-Colloquium in Gießen (Germany) on June 3 1994

It is therefore imperative that (1) the VB be made accessible for logging up to its terminal depth of 4 km and (2) that the HB remain accessible for monitoring the thermal re-equilibration for at least five more years in order to reach the ambitious goals of KTB in respect to an improved understanding of crustal heat transport.<sup>2</sup>

## Thermal data from VB and HB

The thermal measurements in the VB and the HB are summarized in Figs. 1 and 2, respectively. Both figures show (from left to right) temperature  $T$ , vertical temperature gradient (TG)  $\Delta T/\Delta z$ , thermal conductivity (TC)  $\lambda$ , vertical heat flow density (HFD)  $q=\lambda\Delta T/\Delta z$ , and the contribution of radiogenic heat production rate (HPR)  $H$  to  $q$ . In Fig. 2 the next column of the composite log is a profile of rock density  $\rho$ , determined from measurements with a borehole gravimeter (left curve) and on drill chips (right curve). The last column in both figures shows the greatly simplified lithological profiles.

Temperature in the VB is shown by two T-logs (full lines, partially overlapping) and seven BHT-extrapolations (dots). Additionally, the heating and cooling effect of the circulation (above 2300 m and below, respectively) is indicated by hatchure. One log down to 4002 m was recorded in November 1989, 8 months after the end of drilling operations. At that time the drilling-induced thermal disturbances had died out to a great extent, but not yet sufficiently. The second log was recorded after one more year, in December 1990, much closer to thermal equilibrium, but only down to 2 km (for reasons explained above). The BHT-extrapolations are based on repeat measurements in one depth, in part over extremely long times of up to 663 hours. Differences between the logs and these extrapolations reach 1 K at maximum. This is quite a good agreement, considering the strongly simplifying assumptions necessary in BHT-extrapolations.

The difference between the two T-logs results in slightly different vertical temperature gradients in the upper 2 km (Fig. 1, second column). Gradients plotted are computed every 5 m as moving averages over depth intervals of 50 m.

The vertical component of TC (Fig. 1, third column) was determined from measurements on cores in the KTB field laboratory at room temperature. Dots show the measured values which were determined roughly in 5 m intervals. The full line shows the trend which is computed, as in the case of the TG, as a moving average. Hatchure characterizes mean and

---

<sup>2</sup>note in print: the packer has been removed: since November 17 1994 the VB is again accessible to 3996 m.

standard deviation for depth intervals selected according to the simplified lithology (Fig. 1, sixth column).

The fourth column of Fig. 1 shows the vertical component of HFD computed from different methods: The full curve is the product of interpolated TG in column 2 and interpolated vertical TC (at room temperature) in column 3. Hatchure indicates the region defined by the product of a mean TG and the mean TC plus or minus its standard deviation, again for depth intervals selected according to the simplified lithology. The blank center region within the hatchured area indicates the influence of the temperature dependence of TC on the HFD. The two lines marking its boundaries are calculated from incremental "Bullard-plots" (see Clauser & Huenges, 1993), and its left and right margins correspond to a HFD with or without temperature-dependent TC, respectively.

Fig. 2 presents the corresponding results for the HB. The first column shows temperature from the available seven BHT-extrapolations, the 4-km log from the VB and some non-equilibrated partial logs from the HB. The conditions for BHT-analyses are much less favourable in the HB, however, compared to the VB: the diameter of the HB is about three

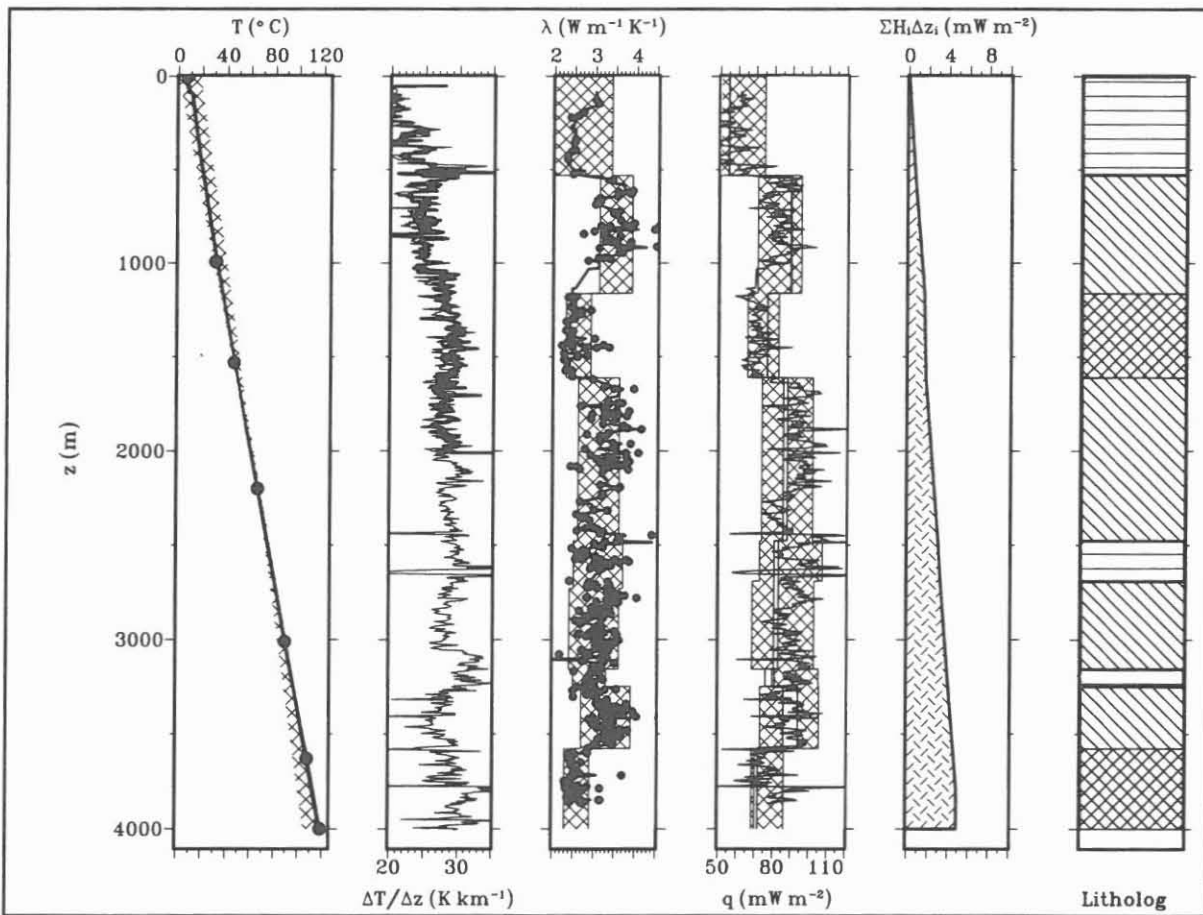


**Figure 1** Thermal data from the KTB-VB; hatchure for lithology: crossed=metabasite, diagonal=gneiss, horizontal=alternating metabasite and gneiss; further details, see text.

times that of the VB, and a maximum shut-in time of only 188 hours was available for an accordingly greater uncertainty of the extrapolations which is indicated in the plot by cross-hatchure. The logs recorded immediately after shut-in indicate the depth intervals which had been heated and cooled, respectively, by the mud circulation.

The following four columns show means and confidence intervals for the vertical TG, TC, and the vertical HFD in depth intervals defined by the BHT-depths, and the cumulative contribution of radiogenic HPR to HFD. In contrast to the VB, very little core was available from the HB, and most measurements were performed on drill chips. As no components can be determined from unsorted chips, TC has to be understood as a statistical mean of all directions of anisotropy. Accordingly, HFD in the fourth column reflects the relatively great uncertainties in TG and TC. Within its uncertainty, the TG is constant and equal to 27-28 K km<sup>-1</sup> over the entire depth interval. It shows no general decrease with depth. The same holds for HFD and its mean of 85 mW m<sup>-2</sup>. The variation which is present seems to correlate rather with the lithological change from metabasite to gneiss due to their distinctly different thermal TC. Because of the steep dip of these rock units this is interpreted as an indication of conductive lateral heat transfer. This interpretation is supported by a comparison of rock

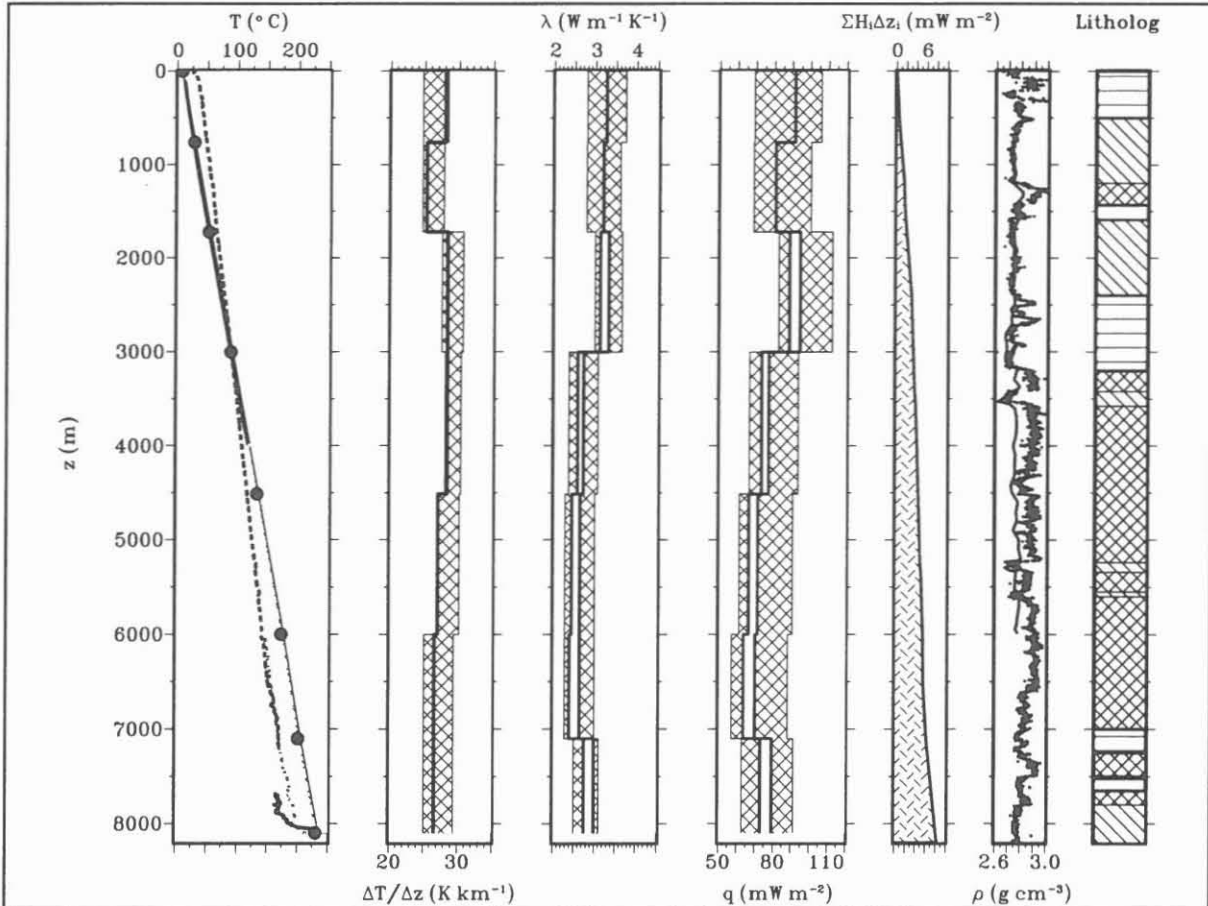


**Figure 2** Thermal data from the KTB-HB; hatchure for lithology: crossed=metabasite, diagonal=gneiss, horizontal=alternating metabasite and gneiss; further details, see text.

density determined in the lab from cores and from borehole gravimetry. While cores represent the density of the drilled section, borehole gravimetry is influenced by the density distribution around the borehole. Column 6 of Fig. 2 shows density determined by the two methods: on the left from the continuous borehole gravimeter and on the right from individual core measurements. Below 3000 m the density of the drilled metabasic material is significantly greater than that from borehole gravimetry, which is more like that of gneiss. The last column, finally, shows again a simplified lithological profile.

### **Which Processes are involved in Crustal Heat Transfer?**

The surprising result from the VB is the increase in HFD by more than 50 % from 52  $\text{mW m}^{-2}$  near the surface to 83  $\text{mW m}^{-2}$  below a depth of about 500 m. The temperature prediction prior to the drilling of the VB was certainly greatly impaired by this fact, since the geothermal site-investigation was based exclusively on data from boreholes shallower than 500 m (Burkhardt et al., 1989). The unexpected increase in mean vertical HFD could be explained essentially by three processes: (1) refraction of vertical heat flow by strong lateral contrasts in TC, (2) reduction of the HFD near the surface by groundwater recharge in a regional, topography-driven flow system, and finally (3) reduction of the TG near the surface by diffusion of climatically induced variations of the mean annual temperature at the earth's surface (see Jobmann & Clauser, 1994).

Results from the HB are surprising as well: the TG in 8.1 km depth is still  $28 \text{ K km}^{-1}$ , and no decrease with depth could be observed so far. HFD at this depth amounts to  $77 \pm 13 \text{ mW m}^{-2}$ . Assuming a constant radiogenic HPR of  $1 \mu\text{W m}^{-3}$ , a one-dimensional (1D) extrapolation of this HFD to 30 km depth yields a range of 43-68  $\text{mW m}^{-2}$ . This corresponds to temperatures above 800 °C, even taking into account the uncertainty in the mean crustal TC assumed in the extrapolation. At this temperature acidic to intermediate crustal rocks are already past their solidus (see e. g. Thompson, 1992). Seismic results, however, give hardly any clues for the existence of partial melts in the lower crust beneath the KTB. Therefore, temperatures as high as this are not very probable in these crustal depths. For this reason a further decrease of HFD with depth is generally expected. This could come by an increase in the presently observed HPR or by additional heat sources below the present depth. However, only transient processes are suitable for this such as sub-recent volcanism/plutonism or exothermal liberation of bonding energy by hydration of acidic crustal rocks. It seems little probable that one of these two processes, having been active in the geological past, can account for the HFD variation observed today (Huenges et al., 1994). Convection of fluids in

the whole crust and also channelling of the regional conductive heat flow by lateral heterogeneity in TC could well lead to the observed relatively high TG. However, the open questions in this context cannot be definitively clarified at present due to the completely inadequate data base. However, numerical simulations provide some insight, and give clues to the crustal permeabilities, TC distributions, and basal HFD required in each case.

## **Numerical Simulations**

This review merely summarizes main results. Many details of the simulations reported can only be touched briefly. More detailed descriptions are found in the original papers referenced. All 2D-vertical cross-sectional models implement impermeable vertical boundaries for the simulation of fluid and heat flow. Depending on the model, the top boundary condition in respect to hydraulic head (or pressure) and temperature is chosen as constant or laterally variable. At the bottom all models are impermeable in respect to flow, and either temperature or HFD are specified.

Results, in part preliminary, will be presented for the following questions: (1) Is it possible to reconstruct transient temperature variations at the earth's surface from temperature logs? (2) Is the conductive, vertical heat flow refracted by lateral heterogeneities in TC, or is heat advectively redistributed by convection systems in the upper crust? (3) Do the Franconian lineament or the Eger graben (a fault zone and a graben system close to the KTB) possibly serve as preferential flow-zones for fluids from depth? (4) What is the distribution of heat sources in the middle and lower crust, and what are the thermal consequences of the Erbdorf body (a seismically identified structure at depth)?

### **Clues for Temperature Variations at the Earth's Surface from Temperature Logs?**

Due to the low thermal diffusivity of rocks variations in time of the earth's surface temperature are preserved in temperature logs from boreholes. Thus it is possible, at least in principle, to reconstruct the paleo-temperature at the earth's surface from T-logs. Analyses of the VB's most equilibrated temperature log yield results that are compatible with current knowledge about European climatic history, such as the end of the most recent (Würm) glaciation roughly 12000 years ago (Clauser & Huenges, 1994). However, presently the existing data do not sufficiently discriminate between such a paleoclimatic and one of the following interpretations.



material	$\lambda$ , $\text{W m}^{-1} \text{K}^{-1}$	H, $\mu\text{W m}^{-3}$
sediments	2.0	0.4
gneiss	2.6 / 3.9	1.5
metabasite	2.5	0.8
granite	3.7	6.0
middle crust	3.4	0.6 - 1.0

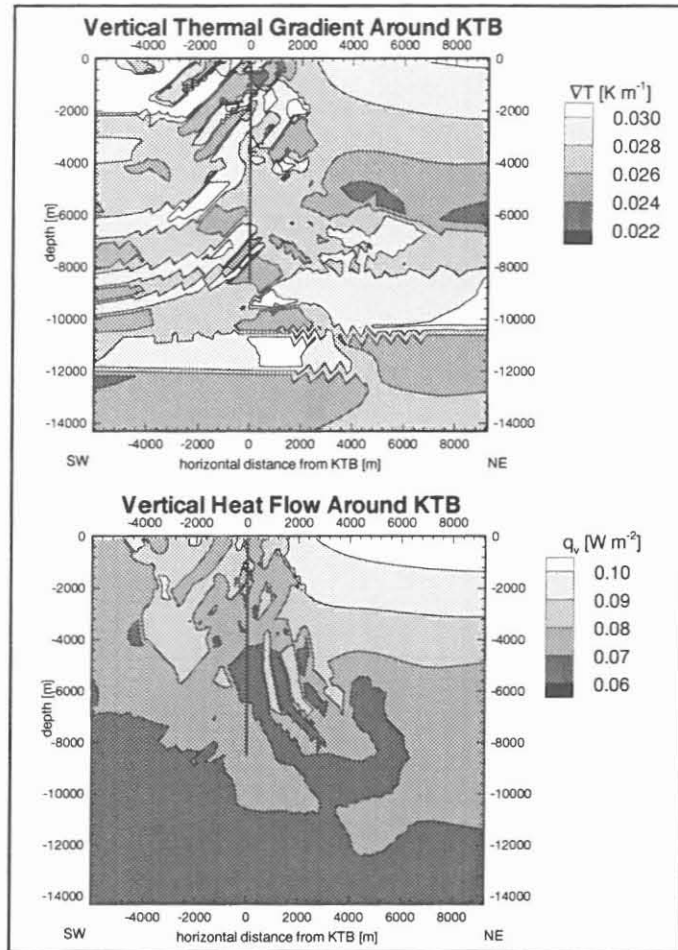


**Table 1** Thermal conductivity  $\lambda$  and heat production rate H for model in Fig. 3. Thermal boundary conditions are a temperature of 7.4 °C at the surface and 440 °C in 16 km depth.

**Figure 3** Temperature gradient and vertical HFD below the KTB, in a conductive simulation based on the cross-sectional geologic model of Hirschmann (1993).

### Refraction of Conductive Heat Flow in the Upper Crust?

Already the geologic map of the KTB area indicates an alternation of metabasic and gneissic units, which is also reflected in the drilled profile of the VB and HB. As these units are steeply dipping and due to their contrast in TC of about 25 % there will be a refraction of the otherwise predominantly vertical heat flow. Fig. 3 shows model results based on detailed geological cross-sections (Kohl & Rybach, 1994). The thermal parameters of this simulation are listed in Table 1. According to this result the HFD field around the KTB is mainly characterized by the contrast in TC between the steeply dipping rock units. Similar vertical variations in HFD were observed in the KTB boreholes (Huenges & Zoth, 1991, Clauser & Huenges, 1993). However, advection driven by upper-crustal convection systems is an alternative heat transport mechanism .

### Hydrothermal Redistribution of Heat by Convection in the Upper Crust?

Both forced and free convection will be discussed as driving forces, due to topography and to density contrasts, respectively (Jobmann & Clauser, 1994). As an example, Fig. 5 shows the result of a simulation where permeability decreases from  $2.5 \cdot 10^{-17} \text{ m}^2$  to  $10^{-18} \text{ m}^2$  below 4.8 km depth. Fig 4 shows the simplified schematic subsurface structure and Table 2 the parameter values used in this simulation.

model domain	$\lambda, \text{ W m}^{-1} \text{ K}^{-1}$	$H, \mu\text{W m}^{-3}$	$\theta, \%$	$k, 10^{-15} \text{ m}^2$
1: gneiss	3.3	1.5	1	0.025, 0.001
2: metabasite	2.6	0.6	5	0.5, 0.05
3: granite	3.0	6.0	3	0.25, 0.025
4: sediments	2.2	0.4	15	10
5: gneiss + 2% graphite	4.5	1.5	5	0.1
6: air	0	0	-	-
Erbendorf body (for Fig. 7)	3.3	6.0	1	0.001

**Table 2** Parameters for model in Fig. 4: thermal conductivity  $\lambda$  (at room temperature), heat production rate  $H$ , porosity  $\theta$ , and permeability  $k$  (lower value below 4.8 km depth).

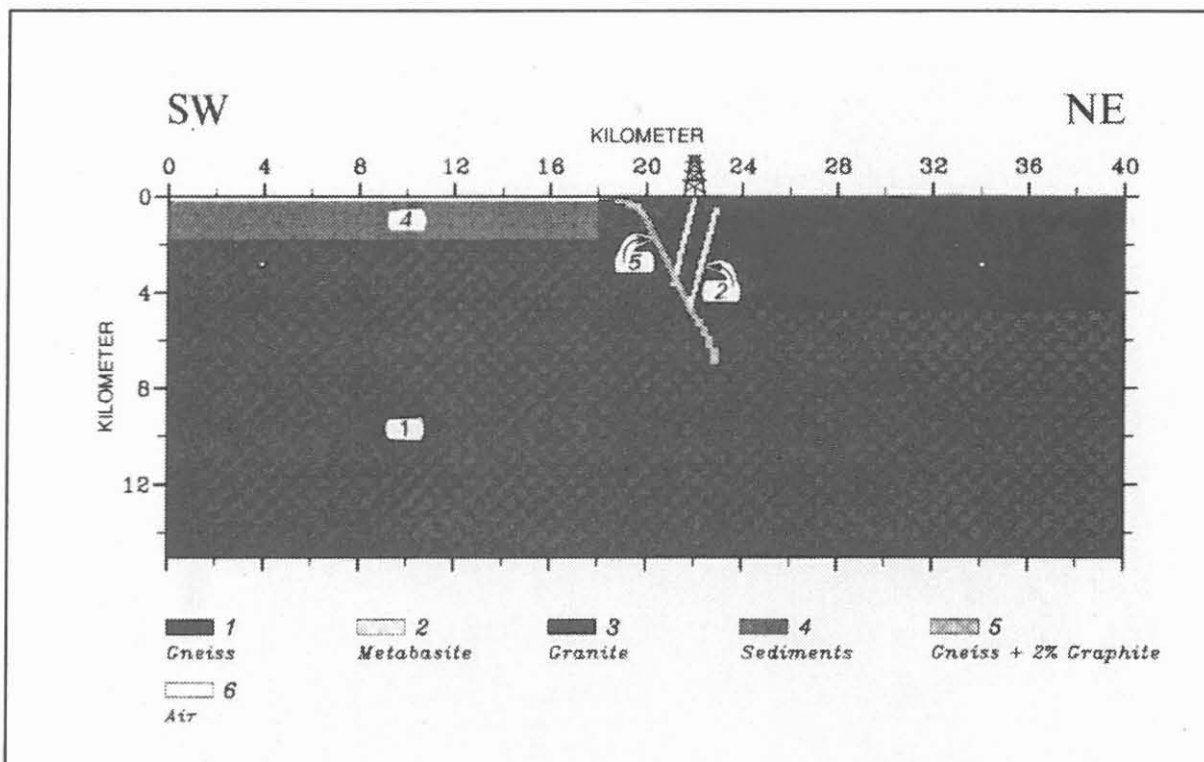


**Figure 4** Simplified geological cross-section of the KTB area - parameters see Table 2.



**Are the Franconian Lineament and the Eger Graben Preferred Pathways for Fluids?**

In Figs. 4 and 5 the Franconian Lineament (FL) and its seismically substantiated possible extension in the upper and middle crust are modelled as zone no. 5. Because of the elevated TC of zone no. 5 (Table 2), HFD is increased in this model region in respect to its surroundings. Thus the FL might serve as a (good) thermal conductor to the middle crust.

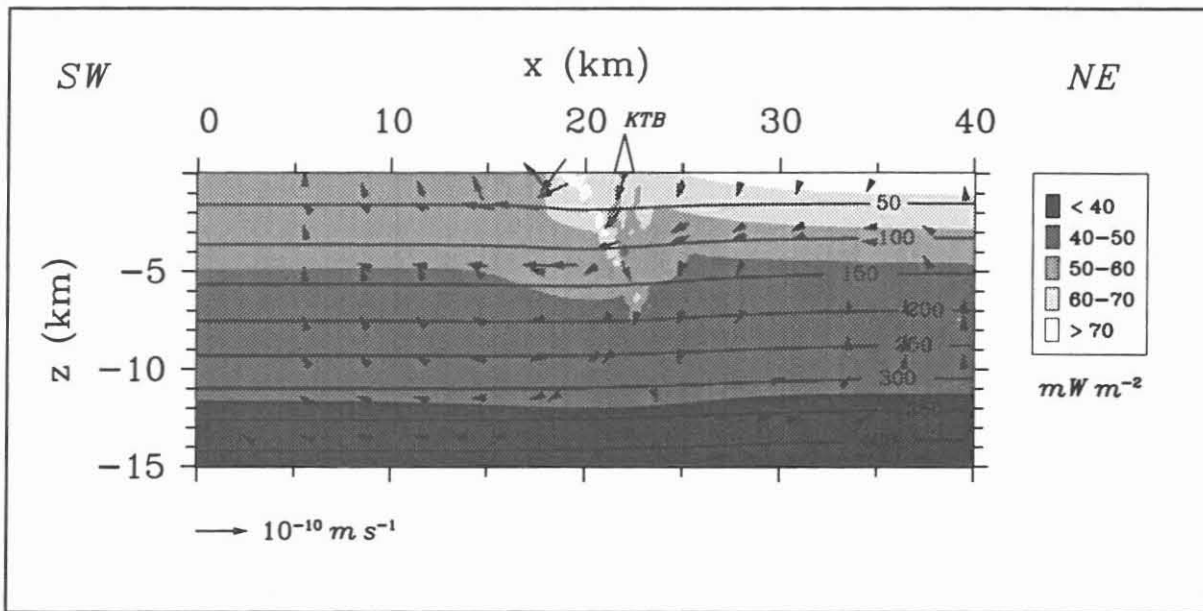


**Figure 5** Distribution of temperature (isolines, °C), HFD (shading,  $mW m^{-2}$ ) and specific discharge (arrows) in the cross-sectional model of Fig. 4. Arrows are scaled in such a way that a doubled length corresponds to a ten-fold specific discharge.

depth, km	0-3	3-12	12-13	13-20
$\lambda, W m^{-1} K^{-1}$	3	3	3	3
H, $\mu W m^3$	1.5	1.3	1.2	1.2-0.6
k, $10^{-15} m^2$	1	0.001	0.000001	0.01
salinity, mol	0	3	3	3

**Table 3** Parameters for model in Fig. 6: thermal conductivity  $\lambda$  (at room temperature), heat production rate H, porosity  $\theta$ , permeability k, and salinity in molar concentration.

Subrecent basic volcanism, a potential additional heat source, is reported from the region of the Eger graben, 20 km to the northeast of the KTB. For modeling purposes an impermeable layer is assumed in the middle crust. Permeability is further assumed to decrease with depth due to the increased mechanical load and to more frequently filled fractures. Acting contrary to this is the increase of thermally induced stresses which might give rise to increased

permeability below 13 km depth. This would facilitate advective heat transfer in the middle crust. Based on the parameters of table 3 and for a basal hHFD of  $100 \text{ mW m}^{-2}$  below the Eger graben and  $20 \text{ mW m}^{-2}$  everywhere else, this results in the T- and HFD-distributions shown in Fig. 6 (Kohl & Rybach, 1994). The main result is a SW-NE trend in HFD in the middle crust which is dissolved near the surface by topographically induced convection systems.

### Additional Heat Sources in the Middle Crust and Implications of the Erbendorf Body?

Other distributions of heat sources in the crust than those discussed so far are conceivable and compatible with the thermal data from the HB. For instance, the following model examines the potential role of the Erbendorf body in heat transfer. It is a seismically identified structure of 2 km thickness and 10 km width situated between 10-13 km below the KTB. For an according extension of the model structure shown in Fig. 4, a satisfactory fit of model results to T and HFD data from the HB requires a basal HFD of  $30 \text{ mW m}^{-2}$  in 30 Km depth and an increased HPR of  $6 \mu\text{W m}^{-3}$  within the Erbendorf body itself. Results are shown in Fig. 7. More details are discussed in the poster contribution by Lehmann & Clauser (1994) in this volume. However, at present there are no specific clues other than this to such a high HPR in the Erbendorf body.

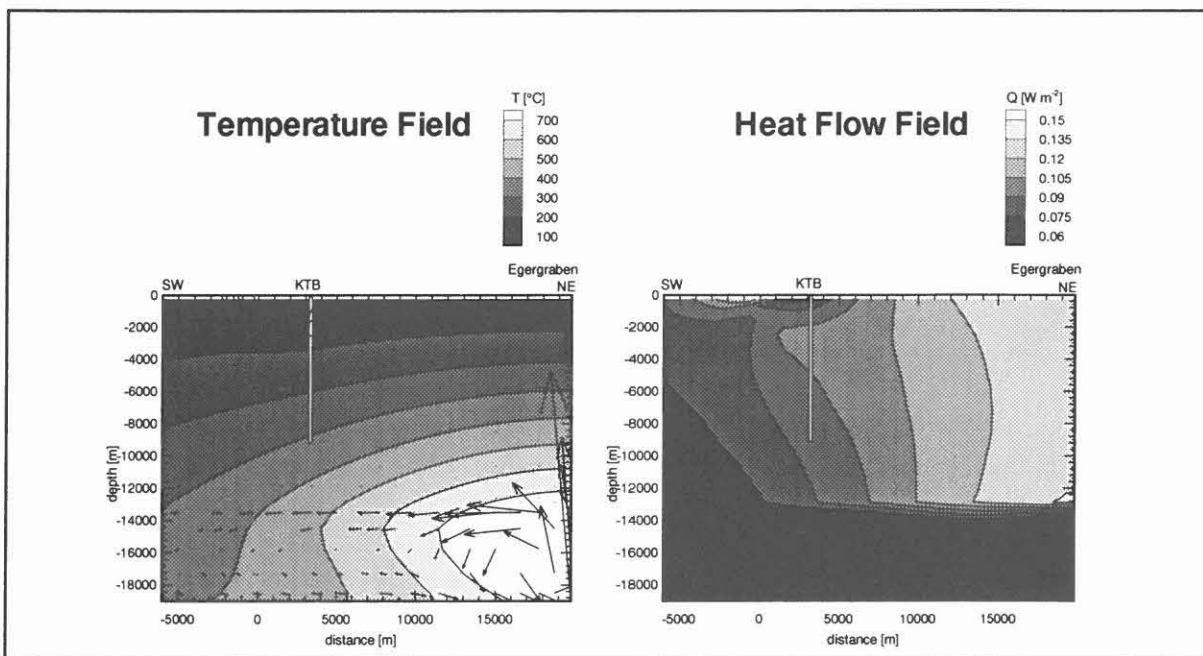


**Figure 6** Simulated temperature and vertical HFD in the middle and lower crust around the KTB - parameters see Table 3.

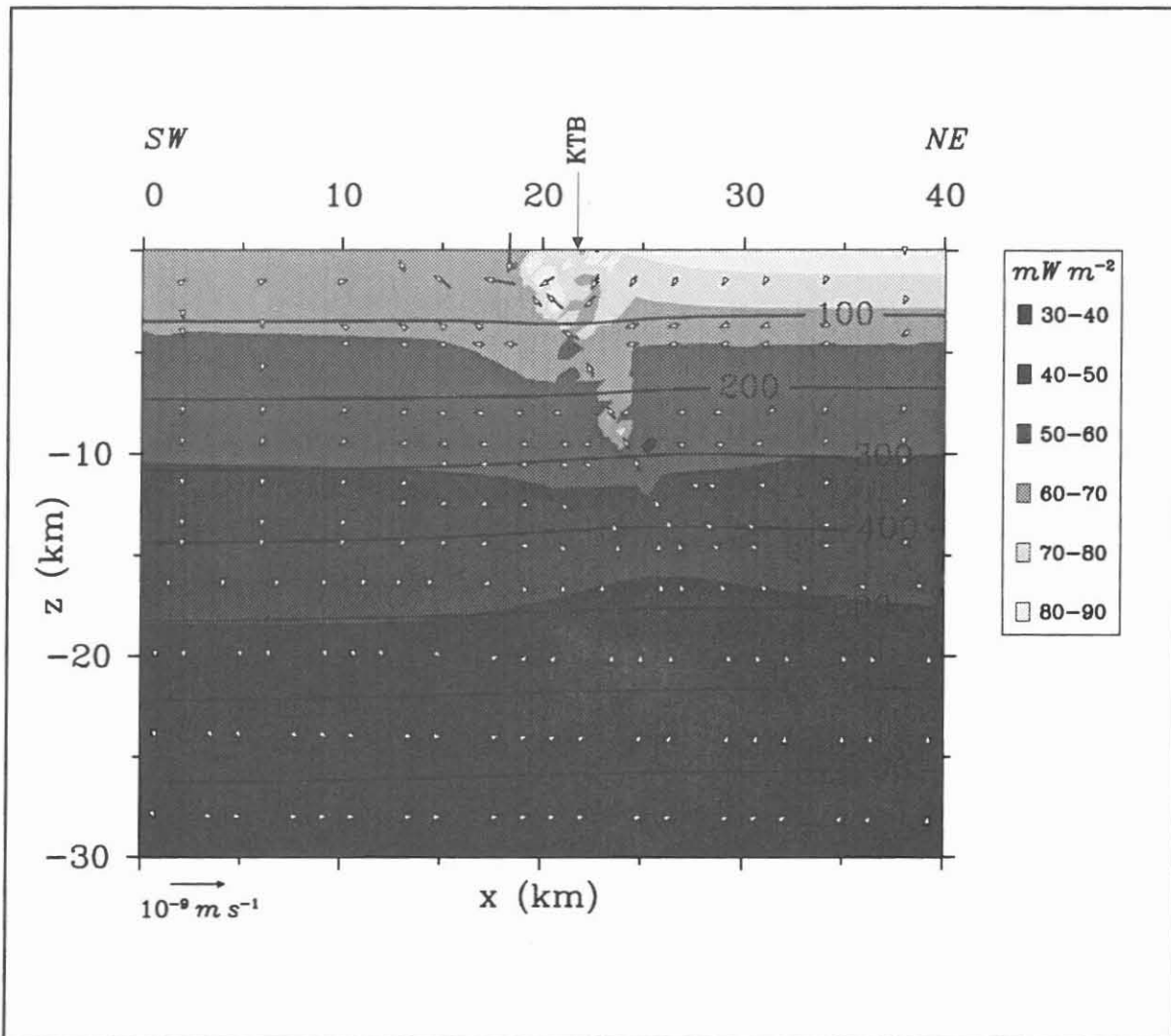


**Figure 7** Distribution of temperature (isolines, °C), HFD (shading,  $\text{mW m}^{-2}$ ) and specific discharge (arrows) in a cross-sectional model like the one in Fig. 4, enlarged to 30 km depth (details see text). Arrows are scaled in such a way that a doubled length corresponds to a ten-fold specific discharge.

## Summary

Temperature data from the KTB-VB and KTB-HB show a uniform TG between 2-8 km depth of  $27\text{-}28 \text{ K km}^{-1}$ . Particularly this but other thermal observations as well furnish boundary conditions for numerical models of heat transport mechanisms. It can be demonstrated that variations of the earth's surface temperature with time can be reconstructed from HB temperature logs, and that the vertical conductive HFD is refracted by lateral heterogeneities in TC. The thermal implications of the following points was further examined by numerical models: (1) the effect of a topographically driven convection system in the upper crust on the HFD distribution, (2) the potential role of the Franconian lineament and the Eger

graben as preferred conduits for fluids, (3) the effect of a forced convection system from the Eger graben to below the KTB via a permeable but confined middle crust, and (4) the distribution of heat sources in the middle and lower crust, in particular the consequences of the Erbendorf body as a high-heat-production structure.

## References

- Burkhardt, H., Haack, U., Hahn, A., Honarmand, H., Jäger, K., Stiefel, A., Wägerle, P. & Wilhelm, H., 1989. Geothermal investigations at the KTB Locations Oberpfalz and Schwarzwald, in *The German Continental Deep Drilling Program (KTB): Site-selection Studies in the Oberpfalz and Schwarzwald*, pp. 433-480, Hrsg. Emmermann, R. & Wohlenberg, J., Springer Verlag, Berlin.
- Clauser, C. & Huenges, E., 1993. KTB thermal regime and heat transport mechanisms - current knowledge, *Scientific Drilling*, 3(6), 271-281.
- Hirschmann, G. 1993. Zur Geologie der KTB-Oberpfalz.- *Z. geol. Wiss.*, 21 (1/2), 105-116.
- Huenges, E. & Zoth, G. 1991. KTB Oberpfalz: temperature, thermal conductivity, and heat flow density. *Scientific Drilling* 2, 81-89.
- Huenges, E., Harms, U., Clauser, C. & Pribnow, D., 1994. Observed Temperature and Heat Flow Density in the KTB: Possible Sources and Tectonic Implications, Proc. VII. Internatl. Symposium on the Observation of the Continental Crust Through Drilling, 25. - 30. 4. 1994, Santa Fe, NM., pp. 118-121, DOSECC Continental Scientific Drilling Program, Texas A&M Univ., College Station, Tx. (USA).
- Jobmann, M. & Clauser, C., 1994. Heat advection versus conduction at the KTB: possible reasons for vertical variations in heat flow density, *Geophys. J. Int.*, 119(1), 44-68.
- Kohl, T. & Rybach, L., 1994. Modelling the Heat Flow Field in the Surroundings of the KTB Site, Proc. VII. Internatl. Symposium on the Observation of the Continental Crust Through Drilling, 25. - 30. 4. 1994, Santa Fe, NM., pp. 114-117, DOSECC Continental Scientific Drilling Program, Texas A&M Univ., College Station, Tx. (USA).
- Lehmann, H. & C. Clauser, 1994. Simulation von Strömung und Wärmetransport an der KTB bis zur MOHO.- This Report.
- Thompson, A. B., 1992. Metamorphism and fluids, in *Understanding the earth*, pp. 222-248, Hrsg. Brown, G., Hawkesworth, C. & Wilson, C., Cambridge University Press, Cambridge.